

PAPER • OPEN ACCESS

Characterization of a precision modular sinewave generator

To cite this article: J Kučera *et al* 2020 *Meas. Sci. Technol.* **31** 064002

View the [article online](#) for updates and enhancements.

You may also like

- [Lung heterogeneity and deadspace volume in animals with acute respiratory distress syndrome using the inspired sinewave test](#)
Minh C Tran, Douglas C Crockett, Federico Formenti et al.
- [The Dwarf Nova V893 Sco Does Not Have a Giant Planet](#)
Bradley E. Schaefer and Franz-Josef Hamsch
- [Liquid metal droplet-enabled electrocapillary flow in biased alternating electric fields: a theoretical analysis from the perspective of induced-charge electrokinetics](#)
Yukun Ren, Rui Xue, Weiyu Liu et al.

Characterization of a precision modular sinewave generator

J Kučera^{1,2} , J Kováč^{1,2}, L Palafox³ , R Behr³  and L Vojáčková¹

¹ Czech Metrology Institute (CMI), Okružní 31, 638 00 Brno, Czech Republic

² Department of Measurements, FEE, Czech Technical University in Prague (CTU), Technická 2, 166 27 Prague 6, Czech Republic

³ Physikalisch-Technische Bundesanstalt, Bundesallee 100, 38116 Braunschweig, Germany

E-mail: jkucera@cmi.cz

Received 11 October 2019, revised 13 January 2020

Accepted for publication 23 January 2020

Published 12 March 2020



Abstract

At the Czech Metrology Institute (CMI) we have developed a precision modular sinewave generator for impedance ratio bridges. The generator was developed to improve previously available designs regarding amplitude and phase accuracy, linearity, absolute stability, stability of the ratio between two outputs and harmonic distortion. It generates up to 7 V_{rms} in a frequency range from 1 mHz up to 20 kHz, extendable to 100 kHz with small changes to the filters. The amplitude resolution is better than 0.01 μV V⁻¹ of full scale with an output voltage stability of 0.05 μV V⁻¹/30 min and a stability for the ratio between two outputs of 0.02 × 10⁻⁶ over several hours. The generator can be powered from internal batteries and is controlled via optically isolated connections. The internal clock and voltage references can be replaced by external ones, optically coupled in the case of the clock. In this paper, we discuss experimental results obtained with the generator used as a signal source in digital impedance bridges with relative combined uncertainties from 10⁻⁵ down to 10⁻⁸. The generators have been used in a bridge to drive a quantum Hall resistor in the AC regime. The use of a generator with an AC quantum voltmeter will also be discussed. The generator is not only applicable in the field of AC impedance metrology but also for on-site comparisons of AC quantum voltage standards or, in general, where there is a need for precision voltage sources.

Keywords: signal generator, synthesizer, voltage, calibration, metrology, impedance, AC Josephson effect

(Some figures may appear in colour only in the online journal)

1. Introduction

Sinewave voltage generators play an essential role in many electrical measurements where they serve as a signal source. For various types of impedance bridges, where high stability, high resolution, low inter-channel crosstalk, and traceability to external references are crucial, commercially available generators are the limiting factor [1, 2]. It was assessed that typically generators with better dynamic

parameters show insufficient stability. For example, a generator used in some impedance bridges [3], has 24 bit resolution and a spurious-free dynamic range better than 92 dBc at 1 kHz. However, its applicability is limited by the stability of the voltage ratio, at approximately 10 μV V⁻¹. Moreover, the range of impedance bridges where it can be used is limited by a minimum working load of 600 Ω [4]. The need to go beyond specifications of series produced commercial generators led several laboratories to the development of dedicated techniques, e.g. where high frequency resolution (better than 10 μHz [5]) or improved stability (voltage ratio stability of two outputs up to 0.01 × 10⁻⁶ for 30 min measurements [6]) of output signals was achieved, distortion of sinewave was lowered [7].



Original content from this work may be used under the terms of the [Creative Commons Attribution 4.0 licence](https://creativecommons.org/licenses/by/4.0/). Any further distribution of this work must maintain attribution to the author(s) and the title of the work, journal citation and DOI.

This paper describes in detail the design of a sinewave generator (SWG), beyond previous design reported in [5, 6], with high resolution for amplitude and phase angle, operating from 1 MHz to tens of kHz, and optimized especially for the audio frequency range. Combining advanced electronics with an optimized design, we developed a digital direct synthesis (DDS)-based modular generator with two output channels in each compact module with stability better than $0.1 \mu\text{V V}^{-1}$ over one hour (the ratio stability is around $0.01 \mu\text{V V}^{-1}$ over several hours), a resolution better than $0.01 \mu\text{V V}^{-1}$ of $7 V_{\text{rms}}$ full scale (FS), or 20 Vpp, a programmable refining of spurious-free dynamic range (SFDR) and internal/external clock and voltage references. A battery power option was included to lower noise coupling from the mains and to omit grounding loops for the most sensitive measurements. Such a generator can be applied in circuits dedicated for measurements of impedance standards defined with two- or four-terminal pairs [8]. The performance of the generators has been demonstrated during the development of digital impedance ratio bridges dedicated for primary impedance metrology, where various types of loads are present [9, 10], including quantum Hall effect-based resistance standards [11, 12]. In another application, the generator has been evaluated recently as a possible transfer standard for AC quantum voltmeter comparisons [13].

2. General properties

The general properties of the latest version of the generator (table 1) is the result of an iteration process of improvements since the original design presented in [9]. Previously, only 10 MHz external reference clock was applicable, synchronized sweep and suppression of higher harmonics were not implemented, frequency range was limited from 1 Hz up to 20 kHz. An updated and detailed description follows.

The basic module of the generator is a two-channel voltage source, powered from the mains or optionally from internal batteries for full electrical isolation. It can be controlled in two modes:

- individually from a simple USB to optical fiber converter;
- in connection with an SWG control unit (SCU) for up to four SWG modules. The SCU contains the USB to optical fiber converter, a clock distribution network, and the charger for the batteries. Presently, up to eight signal channels can be controlled simultaneously from a single computer program. Further extension is possible with appropriate modifications.

2.1. Principle of operation

The generator uses DDS and consists mainly of a frequency reference, a field programmable gate array (FPGA), a sine-wave look-up table and five digital-to-analog converters (see figure 1). The frequency reference can be selected either from an external reference clock source (input ExtCLK) or from an internal 50 MHz clock oscillator. The external clock can be driven from a 1, 10 or 20 MHz TTL signal, which is then

Table 1. Properties of the SWG generator (© 2018 IEEE. Updated reprint, with permission, from [9]).

Characteristic	Value
Max. output voltage (FS)	$7 V_{\text{rms}}$
Max. output current	170 mA
Amplitude resolution	$<0.01 \mu\text{V V}^{-1}$ of FS
Phase resolution	2×10^{-7} rad
Absolute voltage stability	$0.05 \times 10^{-6} \text{ V V}^{-1}/30$ min
Rel. voltage ratio stability of chan. A/B	$0.01 \times 10^{-6}/30$ min
Frequency range	1 MHz to 20 kHz ^a
SFDR ^b for sinewave 0.01–7 V_{rms}	>95 dB @ 100 Hz >85 dB @ 1 kHz
Crosstalk between channels A and B ^b	<−150 dB @ 1 kHz <−105 dB @ 100 kHz
Crosstalk between different modules	Not measurable
Reference clock	1/10/20 MHz Ext. or Int.
Sampling rate	1 MHz
Reference DC voltage	10 V_{dc} Int./5–10 V_{dc} Ext.
Duration of the battery operated mode	Up to 8 h

^aOptimized for the kHz range. Extendable up to 100 kHz with a modification of the output filter.

^bWithout sw optimization and load.

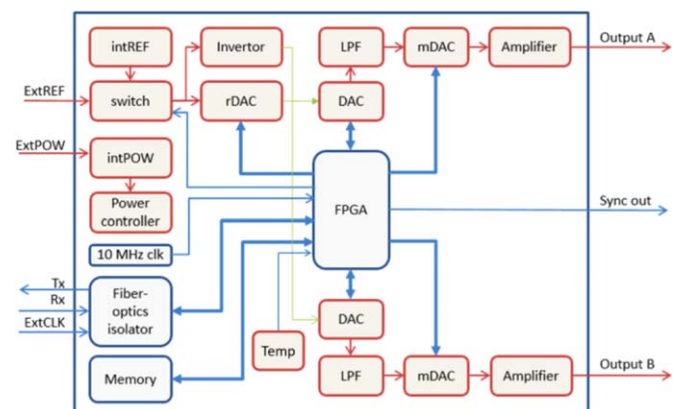


Figure 1. Diagram of the SWG generator with the red blocks related to analog signal paths and blue blocks for the digital signal paths (© 2018 IEEE. Updated reprint, with permission, from [9]).

divided in the module. Synthesized sinewaves show very clean spectra (see SFDR in table 1) due to the combination of the high resolution of the stored sinewave and low clock jitter (the internal clock has a phase jitter lower than 1 ps). Instead of the preprogrammed sinewave, an arbitrary waveform can be stored in the internal memory too.

The two voltage outputs of the SWG share the same DC voltage reference. Therefore, any voltage drift of the reference affects both voltage outputs simultaneously and has no influence on their ratio. This is a crucial property for fully digital impedance ratio bridges, which will be discussed later. The voltage reference for digital-to-analog converters (DACs) can be selected between an internal 10 V (intREF) or a variable external reference (input ExtREF). The temperature of sensitive parts in the module can be monitored with a built-in sensor (Temp).

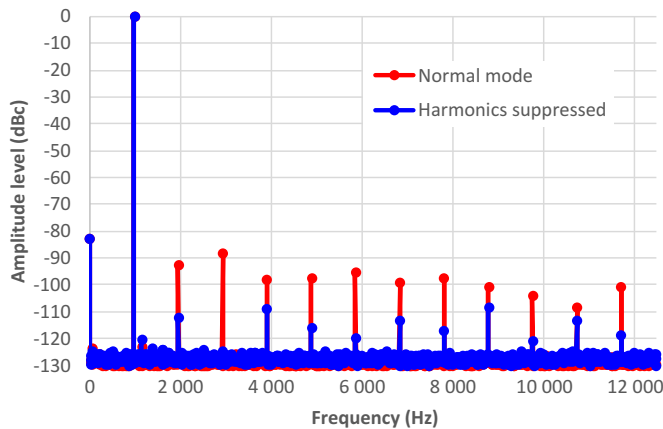


Figure 2. An example of the generator spectrum with and without reduction of the first 11 higher harmonic tones for a 1 V_{rms} signal.

A 20-bit digital-to-analog converter, operating at a sampling rate of 1 MHz, (DAC in figure 1) is used to generate each of the two pure sinewave signals with a fixed output amplitude. A second order low pass filter (LPF) after the DAC removes higher harmonics from the output signal. Then, the output amplitude of the channel is set by an 18-bit multiplying circuit (mDAC), followed by a power amplifier based on bipolar transistors. A voltage sense circuit is implemented to suppress potential effects of the output circuit on the signal amplitude.

Including an mDAC as a part of the sinewave generation circuit allows preserving a high spurious free dynamic range (SFDR) even for extremely small output voltages. For critical applications that require pure sinewaves, higher harmonics can be reduced by combining the original signal with a phase shifted replica of the harmonics [14]. An example at 976 Hz is shown in figure 2, where the SFDR was increased from 88 dBc to 108 dBc.

To obtain output resolutions higher than 18 bits, the DAC reference voltage for each output channel can be adjusted within a small range by an additional 16-bit circuit (rDAC) separately. The achieved amplitude resolution of better than $0.01 \mu\text{V V}^{-1}$ of FS is a direct result of the combination of mDAC and rDAC.

The SWG generator includes several measures to protect connected devices from discontinuities in the output signal. Any changes to the output amplitude settings are performed when the signal is crossing zero voltage. Also, phase shifts are continuous and implemented as a frequency sweep over a short time. Continuity of the signal, as shown in figure 3, is paramount when driving inductive impedances or quantum Hall devices, where any injected charges can lead to the degradation or even the destruction of devices. A trigger output or a reference signal to synchronize, for example, a digitizer or a lock-in amplifier is supplied by a TTL signal (Sync out) with the same frequency as the output signal. Different SWG modules can be programmed simultaneously at different frequencies.

The design of a two-channel module is shown in figure 4. All controls and connectors are located on the front panel except for the power supply connectors. The three

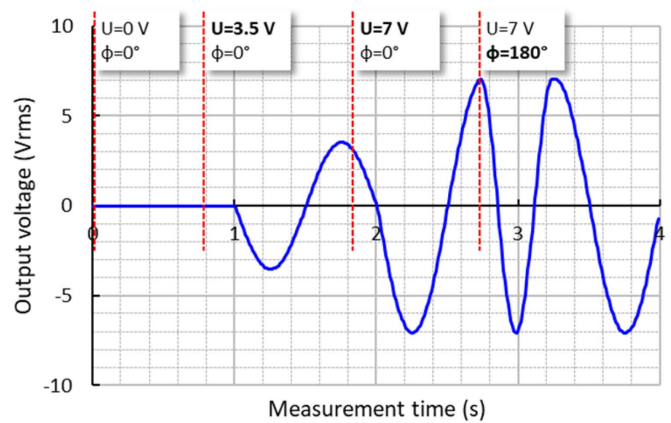


Figure 3. An example for a continuous change of the output signal at 1 Hz frequency, when the amplitude and the phase is modified by a user (the signal was recorded with a DMM 3458A).

BPO/MUSA connectors are used for channels A, B, and an optional ground connection. Communication with the control unit or the computer is performed via fiber optic cables. An external clock reference can be connected to either a fiber optic cable or a BNC input. If desired, an external voltage reference can be used connected using a BNC connector. The generator is powered from an external power supply (extPOW) or an integrated battery pack (intPOW) to minimize crosstalk between SWG modules and the surrounding environment (coupling with other devices via mains power). An integrated switchable active air cooling of all inner parts improves the stability of the output voltage under different loads.

2.2. Stability of the generators

Depending on the target application, both absolute voltage stability (for voltage applications) and the ratio of two output voltages (for impedance bridges) are of interest.

2.2.1. Stability of the output voltage. The absolute stability of the output voltage for a 1 V_{rms} signal (926 Hz) was investigated with PTB's AC quantum voltmeter (its principle is described later in section 4). Figure 5 shows an Allan deviation analysis for three different cases. Firstly, the generator has been temperature stabilized at about 23 °C to $\Delta T = \pm 10$ mK using an MI thermostat chamber.⁴ The results show very good stability of $0.03 \mu\text{V V}^{-1}$ for measurement times of 200–400 s. Even after 1 h, the Allan deviation is at the level of $0.1 \mu\text{V V}^{-1}$. The blue curve shows a similar measurement with the SWG operating in a temperature controlled laboratory (23 ± 1 °C) and shows comparable performance. Due to time limitations an increase of the Allan deviation for the temperature stabilized measurement, observed from about 400 s, was not investigated. As will be discussed in section 4, an external LC filter was also used, but its temperature dependence limited the optimum measurement time.

⁴ Commercial instruments are identified in this paper in order to adequately specify the experimental setup and does not imply recommendation or endorsement by the authors.



Figure 4. View of a SWG generator module without the top cover. Upper: front view—channel A and B outputs (left), communication and clock optical fiber cable connectors (right top), external voltage reference input (center right), status LEDs (bottom right). Lower: rear view—power supply output for custom electronics (middle), fan outlet, charger input (right).

2.2.2. Stability of the voltage ratio. The stability of the ratio between channels A and B in one SWG module was investigated with a coaxial ratio voltage bridge. The reference arms were based on an inductive voltage divider and the second pair of arms was formed from channels A and B. A lock-in amplifier synchronized with the generated voltages was used as the detector in the bridge. Figure 6 shows the Allan deviation analyses of the relative ratio deviation for voltage ratios $N = 1:1$ and $N = 10:1$ with an integration time of 10 s for the lock-in amplifier. In both cases, a level near 0.01×10^{-6} was achieved within 300 s and remained at this level during the whole experiment. The total measurement time was 19 h for the 1:1 ratio and 5 h for the 10:1 ratio.

The long-term stability has been investigated by measuring the ratio between FS outputs of three different SWG modules operating with their internal voltage references and at frequencies up to 2 kHz. The ratios have deviated from their averaged value by less than $6 \mu\text{V V}^{-1}$ over four years.

2.3. Linearity

Since the accuracy of the ratio measurements is directly limited by the accuracy of voltage signals in the reference ratio arms, both the differential and the integral linearity must be known.

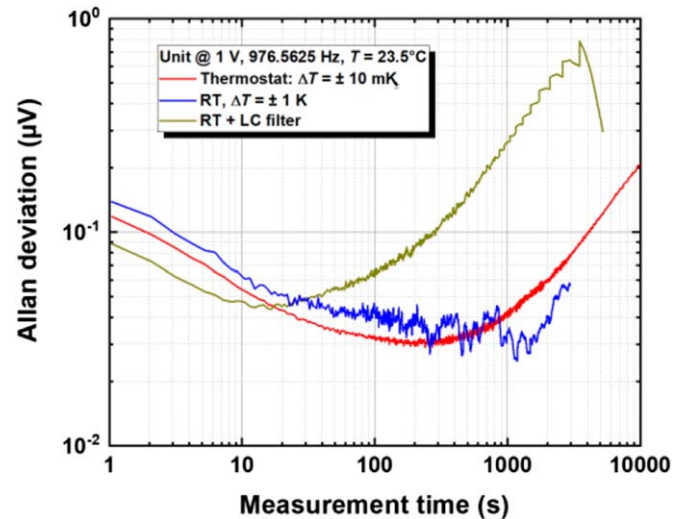


Figure 5. Allan deviation analyses for $f = 976.5625$ Hz and $V_{\text{RMS}} = 1$ V. The generator was temperature stabilized in a thermostat ($\Delta T = \pm 10$ mK) or just in a temperature-controlled laboratory ($\Delta T = \pm 1$ K). In addition, the analysis is shown when the LC filter ($0.1 \mu\text{F}$ – 100 nH– $1.5 \mu\text{F}$) is placed at the output of the device.

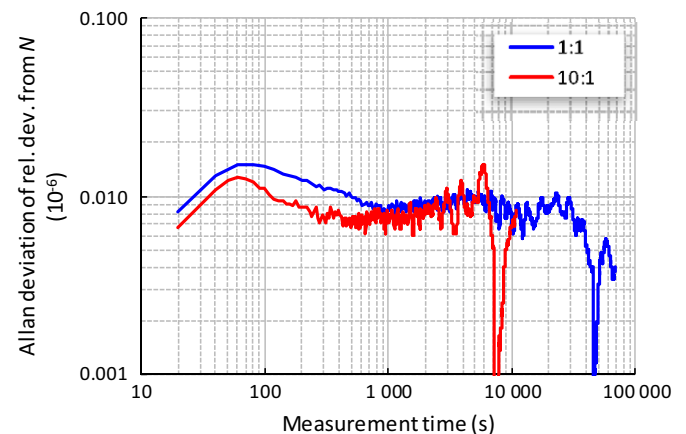


Figure 6. Allan deviation analyses of the relative deviation from ratios $N = 1:1$ and $10:1$ at a frequency of 976 Hz. The generator was in a temperature-controlled laboratory ($\Delta T = \pm 0.5$ K).

2.3.1. Differential nonlinearity. Beside standard linearity tests where a reference digitizer with sufficient linearity is involved, Kučera and Kováč [9]. introduced the idea of testing discontinuities in the output voltage transfer function (differential nonlinearities), and the phase of the generators by means of simple measurements with two generators and one lock-in amplifier. The method is focused on determining the effect of a change in the value of multiple bits on the amplitude and the phase error by evaluating the voltage difference between outputs A and B when mDAC is used to modify the output amplitude of the generator. Such testing is focused on the largest differential nonlinearities. These occur when an increase of the binary code by one least significant bit (LSB) causes a change of multiple bits (e.g. increase of the binary code from 01111 to 10000).

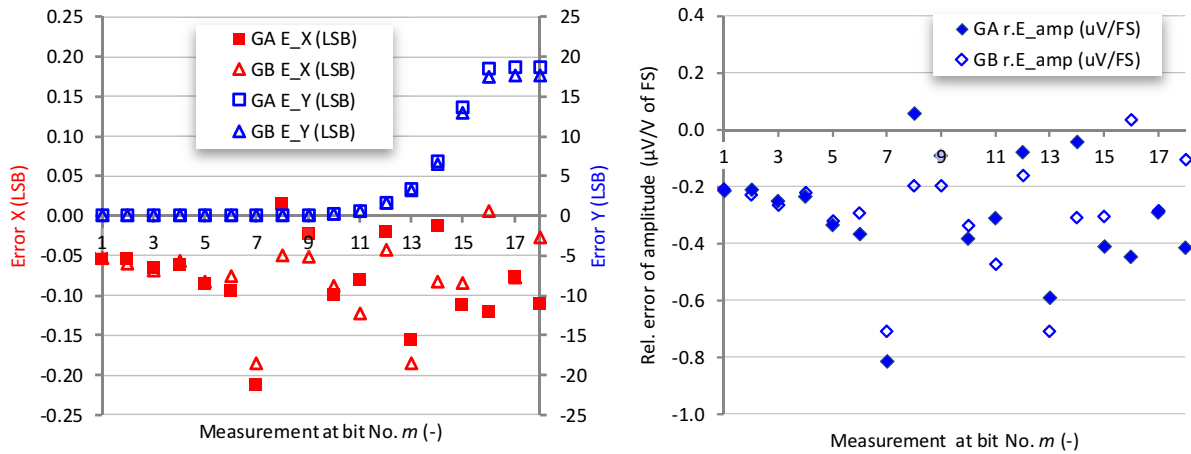


Figure 7. Left: In-phase (E_X) and quadrature (E_Y) voltage errors introduced at 1 kHz in the generator outputs A and B, when the programmed word in the mDAC is changed from $a1[1:m-1] + a0[m:18]$ to $a1[1:m] + a0[m+1:18]$ and from $b1[1:m-1] + b0[m:18]$ to $b1[1:m] + b0[m+1:18]$, respectively, where $a1, b1$ denotes binary ‘1’ and $a0, b0$ denotes binary ‘0’ for channels A and B, respectively. The bit number plotted on the x-axis is the most significant bit which is changed. For example, $m = 5$ corresponds to a change from code 01111 to 10000. Right: Contribution to the relative error of the output voltage amplitude (evaluated from the data in the left graph).

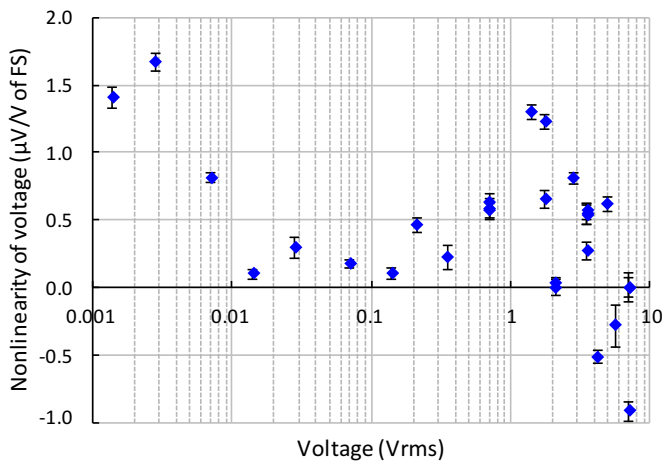


Figure 8. Integral nonlinearity of the output voltage on channel A at a frequency of 1 kHz and relative to the FS voltage. The error bars correspond to the type A uncertainty ($k = 2$).

Such a measurement was repeated with a new SWG generators which has been recently fabricated, i.e. with electronic parts from another fabrication batch, also for the mDAC circuits shown in figure 7. The left graph shows the absolute errors for the two outputs in one module in terms of LSBs, whereas the right graph shows the relative amplitude errors in $\mu\text{V V}^{-1}$ of FS. The new measurements (figure 7 left) produced similar results (compare with figure 8 in [9]). The absolute quadrature error E_Y significantly raises for bits higher than $m = 10$. Nevertheless, the in-phase amplitude raises with 2^m , so the effect of E_Y on the amplitude error is finally small, lower than $1 \mu\text{V V}^{-1}$ of FS at the points tested. The expanded combined uncertainty ($k = 2$) for the amplitude error is finally lower than 0.1 LSB for the in-phase and 5 LSB for the quadrature components of the output voltage.

2.3.2. Integral nonlinearity. One approach to investigate the integral linearity of a generator is to measure the SWG output

using a digitizer with known linearity, where the total rms value or only the amplitude of the first harmonic is evaluated. For the evaluation of the first harmonic amplitude, a digital multimeter (DMM) Agilent 3458A in DCV sampling mode [15] was used. (In the 10 V range, the 3458A matches the full scale output of the SWG). The nonlinearity referred to the FS voltage U_{FS} is equal to $(U_m - U_s)/U_{FS}$, where U_m denotes the measured voltage and U_s the configured voltage. Since we only investigate the linearity of the SWG in this task, we do not need to take care of the absolute accuracy of the DMM, only its linearity is important. Here, we assume that our specific DMM has similar properties as other DMMs of the same type. Josephson AC voltage sources have been used to check their linearity as a function of aperture time [16, 17]. We assume that for an aperture time of 80 μs the integral nonlinearity of our DMM is better than $10 \mu\text{V V}^{-1}$ in the 10 V range for voltages between at least 0.1 and 1 of FS (1 V and 10 V in our case). The results are shown in figure 8 and indicate that the integral nonlinearity of the SWG between 1 mV_{rms} and 7 V_{rms} is smaller than $2 \mu\text{V V}^{-1}$ of the SWG’s FS. The reference transfer function for the integral nonlinearity has a conventional end-point gain correction.

3. The generator as a signal source for digital impedance bridges

Our generators have been used at NMIs (CMI and KRISS) in two types of digital bridges, so called fully digital (FD) and digitally assisted (DA) bridges. These bridges have been reported in depth in [9, 11, 12], so only the operating principles will be repeated here and the measurement results with the SWG presented.

3.1. Fully digital bridges

Figure 9 shows the principle diagram of a fully digital bridge for the ratio measurement of four-terminal pair (4-TP)

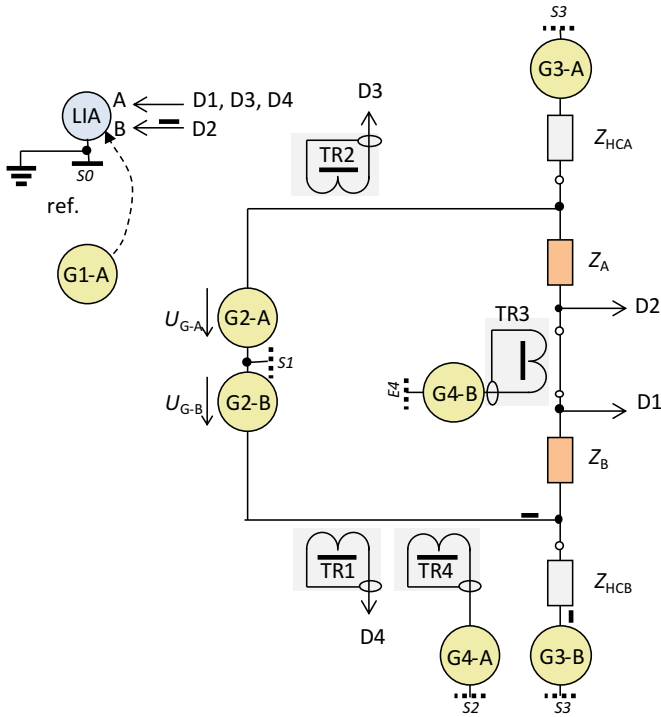


Figure 9. Principle diagram of a fully digital bridge. For simplicity, coaxial wiring is not shown; black rectangles mean coaxial chokes. Same numbers i at points S_i denote grounding points, which are common for paired channels A and B. See the text for the description of the abbreviations.

impedances Z_A and Z_B . The ratio of the two impedances Z_A and Z_B is directly proportional to the output voltages of channels G2-A and G2-B of a reference generator: As a result, the stability of the generators has a direct impact on the performance of the bridge [9]:

$$Z_B/Z_A \approx U_{G2-B}/U_{G2-A}. \quad (1)$$

In accordance with the 4-TP definition, zero currents should flow through the high potential arms of Z_A , Z_B . Hence, the current arms formed by G3-A and G3-B are tuned until the current detectors D3 and D4 read zero. To fulfill the other 4-TP definition condition the voltage between the inner and outer of the low potential (LP) port should be zero. First, G2-B is tuned until the voltage at the Z_B LP port is negligible (point D1). Then, the voltage drop between points D1 and D2 is maintained at a negligible level by means of the injection circuit TR3 with generator G4-B. As a result, the Z_A LP port is also maintained at negligible voltage. All measurement points D_i ($i = 1, \dots, 4$) are connected to a lock-in amplifier (LIA in figure 9) via a coaxial multiplexer. All generators share a common clock and the lock-in amplifier is synchronized from generator G1-A. The relative uncertainty for ratio measurements in such bridges is typically at the level of 10^{-5} and can reach the 10^{-6} level for 1:1 ratios. An additional injection circuit, consisting of transformer TR4 and generator G4-A, reduces relative uncertainties down to the 10^{-7} level.

An example of the stability of the 100 pF:10 pF ratio between two Andeen-Hagerling AH11 capacitance standards

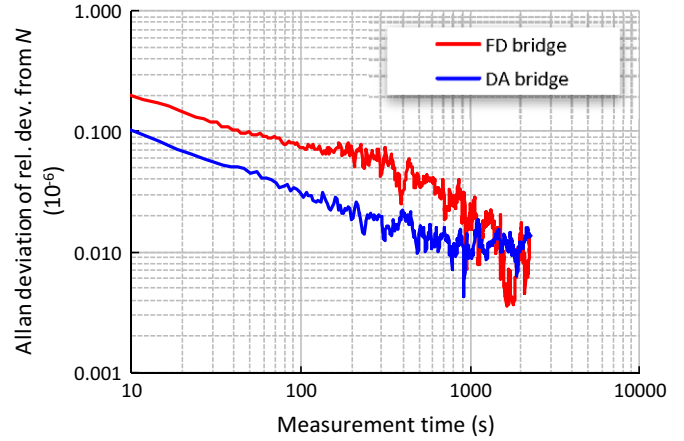


Figure 10. Allan deviation of an $N = 10:1$ ratio measurement using 100 pF and 10 pF capacitors at a frequency of 976 Hz. The bridge voltage for the DA bridge was 1.1 V_{rms} and 3.5 V_{rms} for the FD bridge.

is shown in red in figure 10. By comparison with the measurements with the digitally assisted bridge, the limitation from the properties of the generators used, especially the stability of the A/B voltage ratio stability, become apparent. The Allan deviation becomes smaller than 10^{-7} after 40 s. Within 30 min the level of nearly 10^{-8} is reached. The stability of the whole impedance bridge confirmed in practice the properties of the SWG generators shown in section 2.2.

3.2. Digitally assisted bridges

In comparison to fully digital bridges the reference voltage ratio in digitally assisted bridges is formed by replacing the generators G2-A and G2-B with an inductive voltage divider which shows up to 10 times superior long and short term ratio stability than the SWG generators [9]. The corresponding Allan deviation, in blue, nonetheless demonstrates the good stability of the four SWG modules involved in the bridge circuits. The repeatability of this 10:1 ratio measurement was a few parts in 10^8 within 15 min for both bridges. In the FD bridge, the noise level is approximately two times larger.

3.3. AC QHR bridges

The CMI has selected a DA bridge to measure quantum Hall resistances (QHRs) in the AC regime [18] and for the realization of an AC quantum impedance standard [19], as described in [12] in detail. With the help of continuous changes of the sinewave signals in all synchronized generators, we investigated the shape of the plateau in the AC regime, the longitudinal resistance, and the frequency dependence of the GaAs-based QHR device P743-2-4 (PTB). With the DA bridge, a basic characterization of a double-shielded GaAs-based device can be performed, and the value of the quantum Hall resistance was measured with a relative uncertainty of a few parts in 10^8 . With proper handling nearly flat plateau centers were observed between 1 and 4 kHz with the sample operating at a comparatively high temperature of 4.2 K. The plateau width with a current of 12 μ A was about 0.1 T and remained independent of the

applied frequency. The QHR sample has a frequency dependence of about $0.17 \mu\Omega \Omega^{-1} \text{ kHz}^{-1}$.

4. The generator as a transfer standard for AC quantum voltmeter on-site comparisons

The main parameters for an ideal AC source to be used as a transfer standard for on-site inter-comparisons of quantum voltage standards were listed in previous works [6, 20]. Ideally, the source should provide rms voltages from 10 mV to 7 V, at frequencies ranging from 10 Hz to 2 kHz. The amplitude needs to be stable at least over one set of measurements in the comparison. Phase noise and jitter at its output also affect the repeatability of the results and should be as low as possible. Different AC quantum voltmeters reconstruct the waveform being measured using samples along the period and their results when measuring generators with large to medium levels of harmonic content very strongly depends on the sampling parameters. In particular, the results depend on whether the harmonic content (glitches, residual constant voltage steps on the output) are sampled or not. An ideal transfer standard would generate no harmonic content, so the rms value measured would be independent of what portions of the period are sampled by the two systems [21].

PTB has evaluated the SWG generator as such a transfer standard for on-site comparisons by measuring the stability of the SWG output over the time required in an on-site comparison for one set of measurements. Figure 11 shows the measurement setup including the synchronization setup for the AC quantum voltmeter [22, 23] and the synthesizer. The sampler measures the difference waveform between the output of the SWG and a stepwise approximated 'copy' from the programmable Josephson voltage standard operating at 4.2 K. As the two waveforms are synchronized, the rms amplitude of the SWG output can be calculated from the reconstructed waveform. The difference waveform acquired by the sampler is at least 10 times smaller in amplitude than the reconstructed waveform, which greatly reduced the the influence of sampler errors on the rms measurement of the SWG output.

As described above the spectral purity and the absence of glitches is crucial for sampling measurements. If one of these essential characteristics is missing, different sampling parameters will provide different results and comparisons between different sampling systems or thermal transfer devices cannot be performed at the highest level of uncertainty.

Lee et al [21] have introduced a method to measure the complete curve by sampling a full period in several steps. An equivalent evaluation of glitches and residual steps on the output waveform can be performed by changing the phase angle between the waveform being measured and the Josephson stepwise approximated copy. As the phase angle changes, different portions of the period are used for the measurement of the rms value. The results of such investigation are depicted in figure 12. The visible variation of the rms values with phase for SWG channel 1 (CH1, $\approx 10 \mu\text{V V}^{-1}$ per degree) and SWG channel 2, which included an additional buffer and RC filter, ($\approx 4 \mu\text{V V}^{-1}$ per degree) clearly indicate that harmonics and

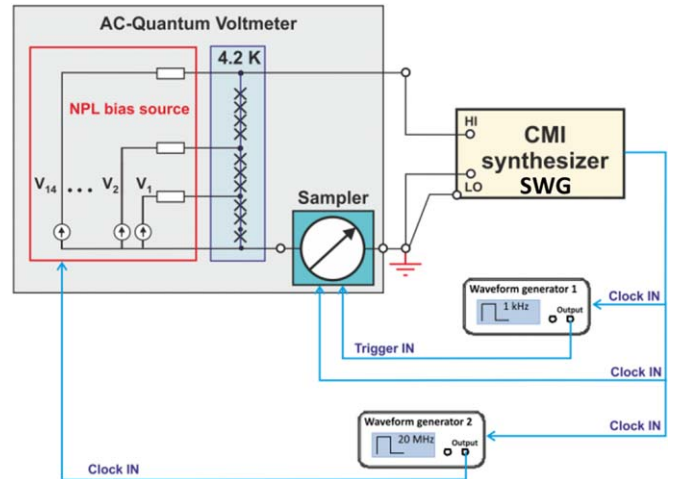


Figure 11. Measurement setup for the characterization of the CMI synthesizer. The blue (dotted) lines show the synchronization signals.

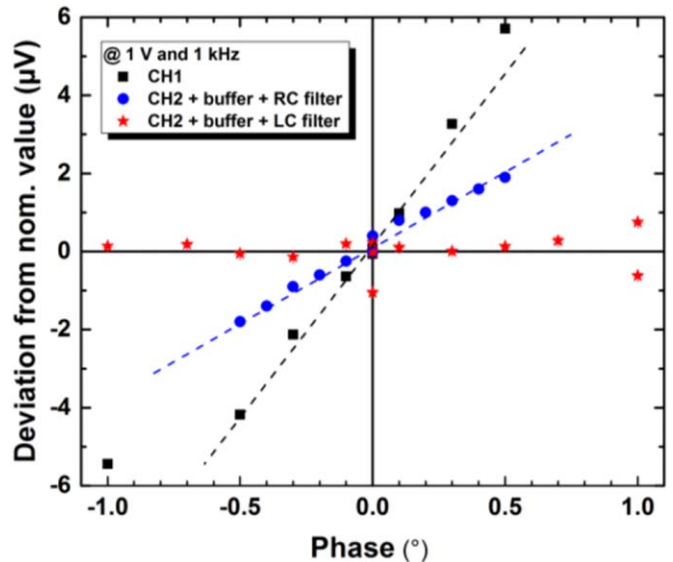


Figure 12. Phase variation with three different output configurations for $f = 976.5625 \text{ Hz}$ and $V_{\text{RMS}} = 1 \text{ V}$.

glitches are an issue for the synthesizer. However, the graph also clearly shows that an external LC filter ($0.1 \mu\text{F}$ – 100 nH – $1 \mu\text{F}$) can reduce this dependence to less than $1 \mu\text{V V}^{-1}$ per degree.

The drawback of using the LC filter is visible in the Allan deviation analysis shown in figure 5 (brown curve), as the stability of the output was greatly reduced. Despite this reduced stability the minimum of the Allan deviation at 5×10^{-8} is already reached after 10–30 s and the level of 10^{-7} after 300 s which would be excellent for an AC voltage transfer device in on-site quantum voltage comparisons. We have further analyzed the stability of the filter by repeating measurements, as shown in figure 13 on the left side for a sweep of the relative phase between -1° and $+1^\circ$. If we correct the measurements for the drift in time, voltage variations remain within $0.1 \mu\text{V V}^{-1}$ for $\pm 0.5^\circ$ phase variation (figure 13 on the right

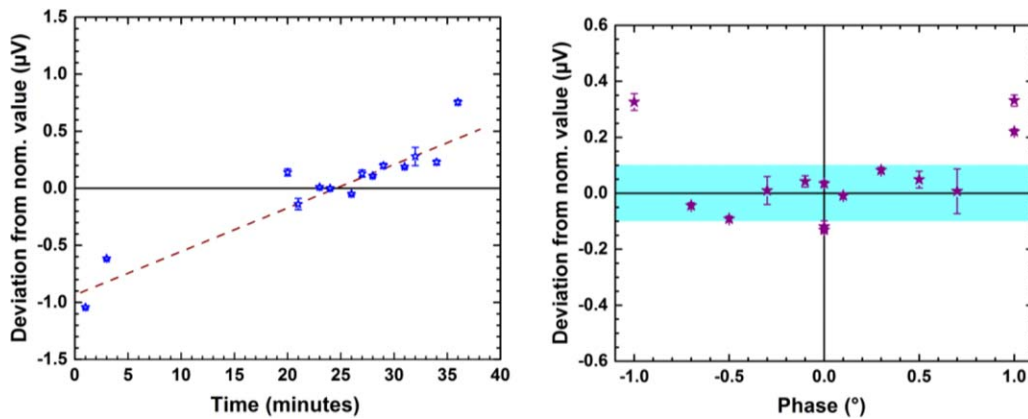


Figure 13. Left: Time trace for $f = 976.5625$ Hz and $V_{\text{RMS}} = 1$ V phase measurements using the synthesizer output CH₂ + buffer + LC filter configuration. Right: Phase dependence for the drift -corrected CH₂ + buffer + LC filter configuration. The shaded area indicates the ± 0.1 μV -range.

side). It seems, that the SWG together with a dedicated filter is a promising alternative for future AC quantum voltmeter comparison.

5. Conclusion

The metrological properties of the sine-wave generator SWG developed at CMI were discussed. Experimental results have shown that it can be a universal tool for building primary impedance calibration setups. Its stability, resolution, spectral purity, synchronization options, output ranges, and optional battery operation have led to digitally assisted impedance bridges with a relative uncertainty down to parts in 10^8 . Fully digital impedance bridges have achieved uncertainties of parts in 10^7 level in the kHz range. For work with quantum Hall-based AC impedance standards, excellent results for the characterization of the Quantum Hall plateaux between 1 kHz and 4 kHz were achieved. Work on the application of the FD bridge for a direct capacitance to resistance traceability chain is ongoing [24]. A possible new application could also be to use the generators with 10 or 20 MHz reference clock in a sampling type bridge.

The amplitude linearity of the two channels in one module was better than $2 \mu\text{V V}^{-1}$ of FS over voltage range from about 1 mV_{rms} up to 7 V_{rms}, and the short-term stability of the ratio between the two channels was up to $0.01 \mu\text{V V}^{-1}$ over 30 min at frequencies around 1 kHz. The long-term stability between different SWG modules was better than $6 \mu\text{V V}^{-1}$ over four years.

In addition to the application in impedance metrology, the suitability of the SWG as a transfer standard for AC quantum voltmeter or Josephson differential sampling on-site inter-comparisons was investigated too. The uncertainty for the measurement of the rms amplitude at 1 V and 1 kHz remained below $0.1 \mu\text{V V}^{-1}$ for measurements of up to one-hour duration. Combined with a simple LC filter, the measured rms value remains independent of the phase angle to the Josephson waveform over 1 degree with uncertainty for the output amplitude of $0.1 \mu\text{V V}^{-1}$. The LC filter, however,

reduced the stability of the output amplitude to three minutes and needs further improvement. Even though there is room to improve the output filter stability, our investigations demonstrate that the CMI generator, together with a dedicated filter, is a promising alternative for future AC quantum voltmeter comparison at the level of parts in 10^7 ($0.1 \mu\text{V V}^{-1}$) or even better.

Acknowledgements

The authors would like to thank J. Grajciar (CMI) and T. Pavlíček (CMI) for consultations and spectral measurements during development of generators.

This work was supported partly by the Joint Research Projects VersICaL (17RPT04) and AIM QuTE (SIB53). These projects have received funding from the EMPIR programme co-financed by the Participating States and from the European Union's Horizon 2020 research and innovation programme. This work was also partly funded by Institutional Subsidy for Long-Term Conceptual Development of a Research Organization granted to the Czech Metrology Institute by the Ministry of Industry and Trade.

ORCID iDs

J Kučera  <https://orcid.org/0000-0003-3209-8594>
 L Palafox  <https://orcid.org/0000-0001-7663-856X>
 R Behr  <https://orcid.org/0000-0002-5480-443X>

References

- [1] Overney F and Jeanneret B 2018 Impedance bridges: from Wheatstone to Josephson *Metrologia* **55** S119
- [2] Kozioł M, Kaczmarek J and Rybski R 2019 Characterization of PXI-based generators for impedance measurement setups *IEEE Trans. Instrum. Meas.* **68** 1806–13
- [3] Overney F, Lüönd F and Jeanneret B 2016 Broadband fully automated digitally assisted coaxial bridge for high accuracy impedance ratio measurements *Metrologia* **53** 918–26

- [4] National Instruments 2008 NI 446x Specifications www.ni.com/pdf/manuals/373770j.pdf
- [5] Callegaro L, Galzerano G and Svetlo C 2001 A multiphase direct-digital-synthesis sinewave generator for high-accuracy impedance comparison *IEEE Trans. Instrum. Meas.* **50** 926–9
- [6] Nissilä J et al 2014 A precise two-channel digitally synthesized AC voltage source for impedance metrology *CPEM 2014 Conf. Digest* pp 768–9
- [7] Zhuang Y, Magstadt B, Chen T and Chen D 2018 High-purity sine wave generation using nonlinear DAC with predistortion based on low-cost accurate DAC–ADC co-testing *IEEE Trans. Instrum. Meas.* **67** 279–87
- [8] Cutkosky R 1964 Four-terminal-pair networks as precision admittance and impedance standards *IEEE Trans. Commun. Electron.* **83** 19–22
- [9] Kučera J and Kováč J 2018 A reconfigurable four terminal-pair digitally assisted and fully digital impedance ratio bridge *IEEE Trans. Instrum. Meas.* **67** 1199–206
- [10] Ortolano M, Palafox L, Kučera J, Callegaro L, D’Elia V, Marzano M, Overney F and Gülmez G 2018 An international comparison of phase angle standards between the novel impedance bridges of CMI, INRIM and METAS *Metrologia* **55** 499–512
- [11] Kučera J and Svoboda P 2018 Development of AC quantum Hall measurements at CMI *CPEM 2018 Conf. Digest*
- [12] Kučera J, Svoboda P and Pierz K 2019 AC and DC quantum Hall measurements in GaAs-based devices at temperatures up to 4.2 K *IEEE Trans. Instrum. Meas.* **68** 2106–12
- [13] Lee J, Schurr J, Nissilä J, Palafox L, Behr R and Kibble B P 2011 Programmable Josephson arrays for impedance measurements *IEEE Trans. Instrum. Meas.* **60** 2596–601
- [14] Analog Devices 2014 AD9912 <http://analog.com> (Accessed 1 May 2014)
- [15] Lapuh R 2018 *Sampling with 3458A* (Ljubljana: Left Right d.o.o.)
- [16] Kurten Ihlenfeld W G, Mohns E, Behr R, Williams J M, Patel P, Ramm G and Bachmair H 2005 Characterization of a high-resolution analog-to-digital converter with a Josephson AC voltage source *IEEE Trans. Instrum. Meas.* **54** 649–52
- [17] de Aguilar J D, Salinas J, Kieler O F and Caballero R 2018 Characterization of an analog to digital converter frequency response by a Josephson arbitrary waveform synthesizer *Meas. Sci. Technol.* **30** 035006
- [18] Ahlers F, Jeanneret B, Overney F, Schurr J and Wood B 2009 Compendium for precise ac measurements of the quantum Hall resistance *Metrologia* **46** R1
- [19] Schurr J, Kucera J, Pierz K and B P K 2011 The quantum Hall impedance standard *Metrologia* **48** 47–57
- [20] Solve S, Bauer M, Behr R, Palafox L, Kim M-S and Rüfenacht A 2018 Towards a BIPM on-site comparison program for AC voltages based on the differential sampling technique *CPEM 2018 Conf. Digest*
- [21] Lee J, Nissilä J, Katkov A and Behr R 2014 A quantum voltmeter for precision AC measurements *CPEM 2014 Conf. Digest* pp 732–3
- [22] Lee J, Behr R, Palafox L, Schubert M, Starkloff M and Böck A C 2013 An ac quantum voltmeter based on a 10V programmable Josephson array *Metrologia* **50** 612–22
- [23] Behr R, Kieler O, Lee J, Bauer S, Palafox L and Kohlmann J 2015 Direct comparison of a 1 V Josephson arbitrary waveform synthesizer and an AC quantum voltmeter *Metrologia* **52** 528–37
- [24] Kucera J and Svoboda P 2020 in preparation